

Light-Particle-Accompanied Fission and the Three-Center Shell-Model*

Josef Hahn, Hans-Jürgen Lustig, and Walter Greiner

Institut für Theoretische Physik der Universität Frankfurt
Frankfurt am Main, Germany

(Z. Naturforsch. **32 a**, 215–222 [1977]; received January 17, 1977)

Light-particle accompanied fission is expected to yield results from which one hopes to learn more about binary scission configurations. As a step in this direction, we present a model that allows the calculation of the probabilities with which a given three-particle setup follows from different binary configurations. First results show the workability of the model.

1. Introduction

About one in every five hundred to a thousand fission events of not too highly excited heavy nuclei is accompanied by the emission of a light charged particle, mostly a ^4He (see e. g. Reference¹). The experiments indicate that most of the α -particles are formed at scission time in the neck between the major fragments. The angular and energy distribution of these light particles and of the fragments should therefore be influenced by the distance, deformations, kinetic energies, and other details of the scission configuration, because all these factors influence the initial Coulomb field which then accelerates the particles to their final states in which they are measured.

After scission, the Coulomb field can be approximated by the mutual field of three point-charges. Within this three-point-charge model, the trajectories can be followed back from the measured distributions to find those starting positions that best reproduce the experiments^{2,3}. This information then helps to learn about pure binary fission as well: Suppose we have a set $\{\alpha\}$ of α -ternary configurations whose wavefunctions form a complete orthonormal basis $\{\Phi_{\alpha T}\}$; the conditional probabilities $p_{b|\alpha}$ that the α -ternary state came from the binary state b is then given by the overlap $|\langle \Phi_{\alpha T} | \psi_B \rangle|^2$. If we take the probability distribution from the three-point charge model and calculate the overlap as described in this paper, we can then calculate the probability to find a certain binary state b in the fission process as $p_b = \sum_{\alpha} p_{b|\alpha} p_{\alpha}$.

* Supported by the Bundesministerium für Forschung und Technologie (BMFT), and by the Gesellschaft für Schwerionenforschung (GSI).

Reprints requests to: Prof. Dr. W. Greiner, Institut für Theoretische Physik der Universität Frankfurt (Main), D-6000 Frankfurt (Main).

The wave functions for the binary states Ψ_B are taken from the two-center shell-model of Maruhn et al.⁴. — The three-center shell-model we used to find $\Phi_{\alpha T}$ is presented in Sec. 2 of this paper. It assumes that the α -particle is created on the line connecting the two major fragments. This assumption is justified by the findings of Fossati and Pinelli³ that the final distribution of the fragments does not depend strongly on the initial distance of the α from this line. — Section 3 describes the calculation of the overlap, details of which can be found in the appendix, while the forth section contains first results.

2. The Three-Center Shell-Model

2.1. The Geometry

The Hamiltonian of the three-center shell-model including spin-orbit- and l^2 -corrections might be represented in cylindrical coordinates in the following manner

$$H = T + V(\varrho, z) + V_{ls} + V_l^2 \quad (1)$$

where T is the kinetic energy and

$$V(\varrho, z) = f \frac{m}{2} \omega_z^2 z'^2 (1 + c z' + dz'^2) + \frac{m}{2} \omega_\varrho^2 (1 + g z'^{n_\varrho}) \varrho^2. \quad (2)$$

Figure 1 shows an example of the geometry described by (2), indicating at the same time the meaning of certain points and intervals on the z -axis. The centers of the nuclear fragments are located at z_A , z_B , and z_C , respectively, z_1 and z_2 being the points at which those fragments join each other, $\lambda = z_B - z_A$, $\mu = z_C - z_B$, $\delta = \lambda + \mu$.

These points define several intervals on the z -axis (e.g. $z < z_A$, $z_A < z < z_1$ etc.). Most of the 'constants'



Dieses Werk wurde im Jahr 2013 vom Verlag Zeitschrift für Naturforschung in Zusammenarbeit mit der Max-Planck-Gesellschaft zur Förderung der Wissenschaften e.V. digitalisiert und unter folgender Lizenz veröffentlicht: Creative Commons Namensnennung-Keine Bearbeitung 3.0 Deutschland Lizenz.

Zum 01.01.2015 ist eine Anpassung der Lizenzbedingungen (Entfall der Creative Commons Lizenzbedingung „Keine Bearbeitung“) beabsichtigt, um eine Nachnutzung auch im Rahmen zukünftiger wissenschaftlicher Nutzungsformen zu ermöglichen.

This work has been digitalized and published in 2013 by Verlag Zeitschrift für Naturforschung in cooperation with the Max Planck Society for the Advancement of Science under a Creative Commons Attribution-NoDerivs 3.0 Germany License.

On 01.01.2015 it is planned to change the License Conditions (the removal of the Creative Commons License condition "no derivative works"). This is to allow reuse in the area of future scientific usage.

	$z < z_A$	$z_A < z < z_1$	$z_1 < z < z_B$	$z_B < z < z_2$	$z_2 < z < z_C$	$z > z_C$
z'	$z - z_A$	$z - z_A$	$z - z_B$	$z - z_B$	$z - z_C$	$z - z_C$
ω_z	ω_{zA}	ω_{zA}	ω_{zB}	ω_{zB}	ω_{zC}	ω_{zC}
ω_ρ	$\omega_{\rho A}$	$\omega_{\rho A}$	$\omega_{\rho B}$	$\omega_{\rho B}$	$\omega_{\rho C}$	$\omega_{\rho C}$
c	0	c_A	c_{B1}	c_{B2}	c_C	0
d	0	d_A	d_{B1}	d_{B2}	d_C	0
g	0	g_A	g_{B1}	g_{B2}	g_C	0
f	1	f_{01}	f_{01}	f_{02}	f_{02}	1
\varkappa	\varkappa_A	\varkappa_A	\varkappa_B	\varkappa_B	\varkappa_C	\varkappa_C
μ	μ_A	μ_A	μ_B	μ_B	μ_C	μ_C

Table 1. Details of the definition of the parameters needed in the three-center Hamiltonian. These values are constants only within each of the z -intervals given.

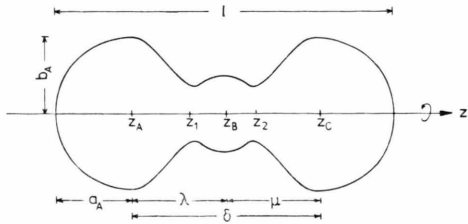


Fig. 1. Configuration described by the three-center Hamiltonian, indicating the meaning of the geometric parameters.

in the Hamiltonian are constant only within each of these intervals while their values might change from interval to interval (see Table 1).

The continuity of $V(\rho, z)$ and the equations

$$V(\rho = 0, z_i) = \varepsilon_i \cdot \frac{m}{2} \omega_z^2 z_i^2, \quad i = 1, 2,$$

that define the height of the barriers between the fragments, determine c , d , and g . – In order to prevent the appearance of additional extrema in the potential $V(\rho = 0, z)$ for low barriers, f had to be introduced. The condition for the appearance of these unwanted extrema is $\varepsilon_i < \frac{1}{6} f_{0i}$.

In addition to ε_i , f_{0i} , and n_g , the free parameters of the model are the ratios of oscillator frequencies

$$P_i = \omega_{z_i} / \omega_{z_A}, \quad i \in \{B, C\}$$

$$Q_i = \omega_{z_i} / \omega_{\rho_i}, \quad i \in \{A, B, C\};$$

the Q_i 's describe the deformation of the individual fragments while the P_i 's are connected with the mass asymmetry. The absolute values of the frequencies are determined by the requirement of volume conservation within the nuclear surface V_0 . For each fragment, Q is connected to the Nilsson deformation parameter β_0 (for the definition see e.g. Ref. 5) by

$$\beta_0 = \sqrt{\frac{4\pi}{5} \frac{1 - Q^2}{2 + Q^2}}.$$

The influence of some of these parameters on the geometry and on the potential along the z -axis is demonstrated in Fig. 2 and Fig. 3 for $Q_B = P_C = 1$,

$Q_A = Q_C$. Figure 4 shows the ‘effective’ frequency $\omega_{\text{eff}}^2 = \omega_\rho^2 (1 + g z'^{n_g})$ as a function of z for different n_g 's.

To facilitate comparisons with other models (such as liquid-drop model or two-center shell-model) the relative neck h and the length l of the nucleus are

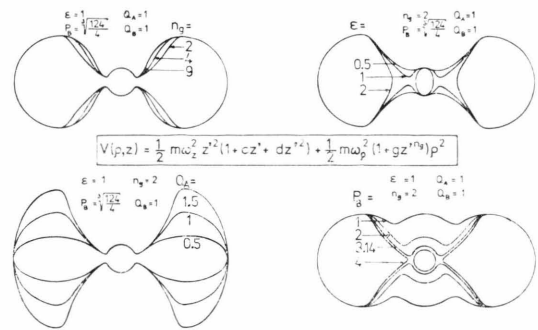


Fig. 2. The three-center configurations given demonstrate the influence of the parameters n_g , ε , Q_A , and P_B on the geometry. $\varepsilon = Q_A = Q_B = Q_C = 1$, $P_B = \sqrt[3]{124/4}$ describes asymptotically the breakup of ^{252}Cf in two equal fragments and one ^4He -particle.

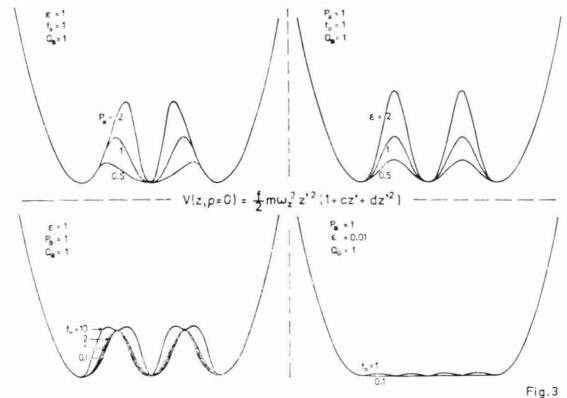


Fig. 3. Influence of the parameters P_B , ε , and f on the potential along the z -axis described by the Hamiltonian (2.1). Note the additional minima in the lower part of the figure that occur if $\varepsilon < f_0/6$.

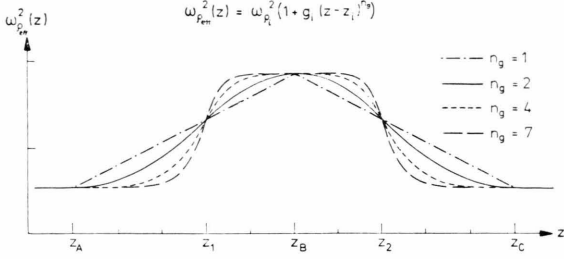


Fig. 4. z -dependence of the effective frequency in the Q -direction $\omega_{\text{eff}}^2(\mathbf{z}) = \omega_{0i}^2(1 + g_i(z - z_i)^{n_g})$ for different values of n_g .

defined as

$$h_{1,2}^2 = \left(\frac{Q(z_{1,2})}{Q(z_i)} \right)^2 = \frac{\frac{2V_0}{m} \frac{1}{\omega_{0i}^2} - \varepsilon_{1,2} Q_i^2 (z_{1,2} - z_i)^2}{\frac{2V_0}{m} \frac{1}{\omega_{0i}^2} [1 + g(z_{1,2} - z_i)^{n_g}]},$$

$$l = \delta + \sqrt{\frac{2V_0}{m} \left(\frac{1}{\omega_{ZA}} + \frac{1}{\omega_{ZC}} \right)}.$$

2.2. Spin-Orbit- and l^2 -Corrections

The spin-orbit potential was taken from Ref. 4 as the commutator

$$V_{ls} = [a, (\nabla V(\mathbf{r}) \times \mathbf{p}) \cdot \mathbf{s}]_+,$$

$$a = -\hbar \kappa / m \dot{\omega}_0.$$

The l^2 -correction has to be chosen such that the matrix element will be symmetric, i.e.

$$\langle n' | V_{l^2} | n \rangle = \frac{1}{2} (\langle n' | \beta l^2 | n \rangle + \langle n | \beta l^2 | n' \rangle) - \langle n' | \frac{1}{2} \beta N(N+3) \delta_{if} | n \rangle,$$

where βl^2 is different for each fragment, such that

$$\beta_i = -\hbar \kappa_i \mu_i \dot{\omega}_{0i}$$

and l_i is the angular momentum relative to the i -th center.

The use of $[\beta, l^2]_+$ does not lead to symmetric matrix elements, because the definitions of l^2 and β are not continuous at z_1 and z_2 , and hence the application of l^2 on β does not give unambiguous and meaningful results. The ansatz $l^2 = (\nabla V \times \mathbf{p})^2$ is excluded by the results of Dickmann⁶, who finds that this ansatz (within the two-center model) leads to energy levels that are too low for heavy, strongly deformed nuclei when n_2 is large. The diagonal term is the same as in Reference 4.

The values of κ , μ , and $\dot{\omega}_0$ are mass- (and thus z -) dependent. This, first of all, necessitates the use

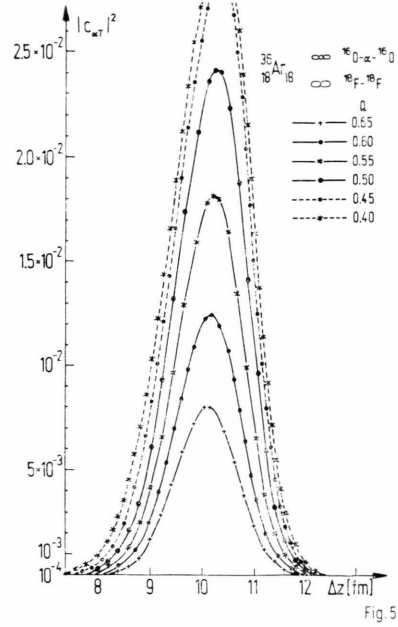


Fig. 5. Square of the overlap c_{aT} between the wave function for the ground state of $^{16}\text{O} - \alpha - ^{16}\text{O}$ (with $Q_A = Q_C = 0.8$, $Q_B = 1$, $\delta = 11.8$ fm) and that for $^{18}\text{F} - ^{18}\text{F}$ as a function of the two-center distance Δz for different deformations $Q \equiv Q_1 = Q_2$ of the ^{18}F 's.

of the anticommutator in V_{ls} since they do not commute with \mathbf{p} and also the explicit definition of the matrix elements of V_{l^2} . Secondly, it forces the assignment of mass values to the individual fragments even before their separation: Each fragment is completed to a spheroid, the volume of which is calculated and used to determine the mass number. — The A -dependence of κ and μ was taken from⁷, while⁵

$$\hbar \dot{\omega}_0 = 41 A^{-1/3} \text{ MeV}.$$

2.3. Diagonalization

Since the Schrödinger equation based on Hamiltonian (1) cannot be solved analytically, H is divided into a term H_0 describing three adjacent oscillators with identical semi-axis in Q -direction, a term H_1 allowing the fragments to have different semi-axis in the Q -direction, a term H_2 with the aid of which the barriers between the fragments are rounded and made variable, and the spin- and angular momentum dependent terms:

$$H = H_0 + H_1 + H_2 + V_{ls} + V_{l^2},$$

$$H_0 = \frac{p^2}{2m} + \frac{m}{2} (\omega_z^2 z'^2 + \omega_{00}^2 Q^2),$$

$$H_1 = \frac{m}{2} [\omega_\rho^2 (1 + g z'^{n_\rho}) - \omega_{\rho_0}^2] \varrho^2,$$

$$H_2 = \frac{m}{2} \omega_z^2 z'^2 [(f-1) + c z' + dz'^2].$$

The eigenfunctions of H_0 can be determined analytically and are used as basis for the diagonalization of H . They can be found by the ansatz

$$\Psi(\varrho, z, \varphi, s) = \eta_{n_\varphi}(\varphi) \chi_{n_\rho}^{[n_\rho]}(\varrho) \psi_{n_z}(z) v_{m_s}(s)$$

where $\eta_{n_\varphi}(\varphi)$ and $\chi_{n_\rho}^{[n_\rho]}(\varrho)$ are given in ⁴ and $v_{m_s}(s)$ is a spinfunction. The equation for $\psi_{n_z}(z)$ has to be solved for each of the intervals $(-\infty < z < z_1)$, $(z_1 < z < z_2)$, and $(z_2 < z < \infty)$ separately. In each of these intervals, it can be reduced to the equation of the Parabolic Cylinder ⁸

$$[d^2/dx^2 - (\frac{1}{4}x^2 + a)] \psi(x) = 0, \quad (3)$$

where $x = \pm \sqrt{2} k_z z'$, $a = -(n_z + \frac{1}{2})$, $k_z = m \omega_z / \hbar$.

The general solution of (3) is a linear combination of $U(a, x)$ and $V(a, x)$ which are defined in ⁸ with the asymptotic behaviour

$$U(a, x) \xrightarrow{x \rightarrow +\infty} 0, \quad V(a, x) \xrightarrow{x \rightarrow +\infty} \infty.$$

Thus, the only meaningful solution is

$$\psi_{n_z}(z) = \begin{cases} A_1 U[a_A, -\sqrt{2} k_{ZA}(z - z_A)] & z < z_1, \\ A_2 U[a_B, \sqrt{2} k_{ZB}(z - z_B)] \\ + B_2 V[a_B, \sqrt{2} k_{ZB}(z - z_B)] & z_1 < z < z_2, \\ A_3 U[a_C, \sqrt{2} k_{ZC}(z - z_C)] & z > z_2. \end{cases}$$

Since the energy for any given level of H_0 ,

$$E_{n_z, n_\rho, n_\varphi} = \hbar \omega_z (n_z + \frac{1}{2}) + \hbar \omega_{\rho_0} (2 n_\rho + |n_\varphi| + 1)$$

has to be the same in all three fragments, we have to take

$$a_B = a/P_B \text{ and } a_C = a/P_C \text{ if we define } a \equiv a_A.$$

$\psi_{n_z}(z)$ and $(d/dz)\psi_{n_z}(z)$ are continuous at $z = z_{1,2}$ only for certain values of a which have to be calculated numerically. $A_{1,2,3}$ and B_2 are determined by the normalization of $\psi_{n_z}(z)$.

With this particular choice of basis functions all matrix elements can be calculated analytically.

3. Calculation of the Overlap

It was pointed out in the introduction that we need to know the conditional probabilities $\{p_{b|\alpha}\}$ as well as the distribution $\{p_\alpha\}$ in order to calculate the probability p_b of finding a binary configuration b during the fission process. While the p_α 's are taken

from the experiment via the three-point charge-model, $p_{b|\alpha}$ is the square of the overlap between the eigenfunctions of the two- and three-center Hamiltonians.

To calculate these overlaps, we make use of the fact that the overlap of any two antisymmetrized N-neutron-Z-proton functions, which depend upon A single particle coordinates

$$\Phi(1, 2, \dots, A) = (1/\sqrt{A!}) \det_A[\varphi_i(j)],$$

$$\Psi(1, 2, \dots, A) = (1/\sqrt{A!}) \det_A[\psi_i(j)]$$

can be written as

$$\langle \Phi | \Psi \rangle = \det_A(\langle \varphi_i | \psi_j \rangle).$$

The eigenfunctions of the three- and two-center Hamiltonians $H^{(3)}$ and $H^{(2)}$ have to be calculated by diagonalization and will therefore be superpositions of N_φ eigenfunctions $\varphi_v^0(\mathbf{r}; P_A, P_B, \omega_{\rho_0})$ of $H_0^{(3)}$ and N_ψ eigenfunctions $\psi_\mu^0(\mathbf{r}; P_1, \omega_{\rho_0})$ of $H_0^{(2)}$, respectively; i.e.

$$\varphi_i(\mathbf{r}; P, Q, \varepsilon, f, n_\rho) = \sum_{v=1}^{N_\varphi} a_{iv}(P, Q, \varepsilon, f, n_\rho, \omega_{\rho_0}) \times \varphi_v^0(\mathbf{r}; P, \omega_{\rho_0}),$$

$$\psi_j(\mathbf{r}; P, Q, \varepsilon, f) = \sum_{\mu=1}^{N_\psi} b_{j\mu}(P, Q, \varepsilon, f, \omega_{\rho_0}) \times \psi_\mu^0(\mathbf{r}; P, \omega_{\rho_0}).$$

Using the abbreviations

$$m_{v\mu} = \langle \varphi_v^0 | \psi_\mu^0 \rangle,$$

$$\hat{A} \begin{pmatrix} 1 & 2 & \dots & A \\ \sigma_1 & \sigma_2 & \dots & \sigma_A \end{pmatrix} = \begin{vmatrix} a_{1\sigma_1} & a_{1\sigma_2} & \dots & a_{1\sigma_A} \\ \vdots & \vdots & \ddots & \vdots \\ a_{A\sigma_1} & a_{A\sigma_2} & \dots & a_{A\sigma_A} \end{vmatrix},$$

and equivalently for \hat{B} and \hat{M} , it is shown in the appendix that

$$\langle \Phi | \Psi \rangle = \sum \hat{A} \begin{pmatrix} 1 & 2 & \dots & A \\ \sigma_1 & \sigma_2 & \dots & \sigma_A \end{pmatrix} \cdot \hat{B} \begin{pmatrix} 1 & 2 & \dots & A \\ \varrho_1 & \varrho_2 & \dots & \varrho_A \end{pmatrix} \cdot \hat{M} \begin{pmatrix} \sigma_1 & \sigma_2 & \dots & \sigma_A \\ \varrho_1 & \varrho_2 & \dots & \varrho_A \end{pmatrix}, \quad (4)$$

where the sum goes over all $\binom{N_\varphi}{A}$ combinations $1 \leq \sigma_1 < \dots < \sigma_A \leq N_\varphi$ and all $\binom{N_\psi}{A}$ combinations $1 \leq \varrho_1 < \dots < \varrho_A \leq N_\psi$.

Furthermore, \hat{M} can be represented by a product of subdeterminants \tilde{M} that combine only basefunctions $\sigma_{\{n_\sigma\}}$ with the same z -projections n_σ of the angular momentum

$$\hat{M} \begin{pmatrix} \sigma_1 & \dots & \sigma_A \\ \varrho_1 & \dots & \varrho_A \end{pmatrix} = \prod_{n_\sigma} \tilde{M} \begin{pmatrix} \sigma_{\{n_\sigma\}} \\ \varrho_{\{n_\sigma\}} \end{pmatrix}.$$

Finally, we make use of the fact that the overlap between a neutron and a proton wave function always vanishes. Thus, $\langle \Phi | \Psi \rangle$ can be split up into

$$\langle \Phi | \Psi \rangle = \langle \Phi_N | \Psi_N \rangle \cdot \langle \Phi_Z | \Psi_Z \rangle,$$

where $\langle \Phi_N | \Psi_N \rangle$ and $\langle \Phi_Z | \Psi_Z \rangle$ are also given by (4), except that N and Z , respectively, have to be substituted for A . N_φ and N_ψ are the respective numbers of base functions.

The integrals involving the φ - and ϱ -variables that occur when the overlaps between the base functions are calculated, can be determined analytically in a straight forward manner, while the z -integrals, involving parabolic cylinder functions with different arguments, have to be integrated numerically. This can be done very fast and accurately with the aid of Gauss-quadrature formulae (for details see⁹).

4. Results

To see whether the theory outlined in the previous sections gives reasonable results, we calculated the probability for ^{36}Ar going from a binary ^{18}F -molecular configuration to an $^{16}\text{O} - \alpha - ^{16}\text{O}$ configuration; the α just touching each of the ^{16}O 's (for a sketch of the configurations see Figure 6). We

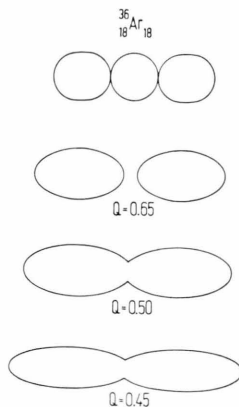


Fig. 6. The three-center geometry as described in the caption of Fig. 5 and three two-center configurations (with $\Delta z = 10.1$ fm) whose wave functions have maximal overlap with $\Phi_{^{16}\text{O}-\alpha-^{16}\text{O}}^0$.

simplified the calculations by taking the basis functions only, i.e. by assuming that $\hat{A} = \hat{B} = \hat{1}$ and $N_\varphi = N_\psi = A$.

These assumptions are probably justified for light nuclei, because the $l s$ - and l^2 -corrections are not ex-

pected to give very large contributions, and the difference between $\omega_\rho(^{16}\text{O})$ and $\omega_\rho(\alpha)$ will be small, especially when the ^{16}O nuclei are given a prolate deformation while the α is taken to be a sphere.

Figure 5 shows $|C_\alpha|^2 = |\langle \Phi_{^{16}\text{O}-\alpha-^{16}\text{O}}^0 | \Psi_{^{18}\text{F}-^{18}\text{F}}^0 \rangle|^2$ for the ground state of $^{16}\text{O} - \alpha - ^{16}\text{O}$ with $Q_A = Q_C = 0.8$, $Q_B = 1$, $\delta = 11.8$ fm and different two-center configurations with $Q \equiv Q_1 = Q_2$ describing the deformation of the ^{18}F 's. As was to be expected from the experimental results (with heavy nuclei), the overlap increases with increasing deformation of the fragments; the probability for the formation of an α -particle is large only near the scission point at $\Delta z \cong 10$ fm. Some of the configurations of maximal overlap are given in Figure 6.

Up to a deformation of about $Q = .5$ ($\beta_0 \cong .53$) the probabilities given are those for the ground state of the $^{18}\text{F} - ^{18}\text{F}$ -molecular-system. For larger deformations ($Q < .5$) and $\Delta z \gtrsim 9$ fm, excited two-center states have to be taken, since the two-center ground state now contains wave functions with an n_φ -quantum number that differs from those of the three-center ground state. The overlap thus vanishes as explained in the appendix. The excitation energies near the maximal overlap are about 3 MeV for $Q = .45$ and 11 MeV for $Q = .4$. — The use of excited two-center configurations probably has no physical meaning, though. Rather, it is due to the fact that we took basis functions only. The overlap between the ground states of the total Hamiltonians, which, especially, round the edges where the fragments are joint together, most probably will not vanish, because the ‘excited’ basis states are then mixed into the ground states.

Using three ^{12}C nuclei in contact (see insert of Fig. 7) and the same two-center configurations as

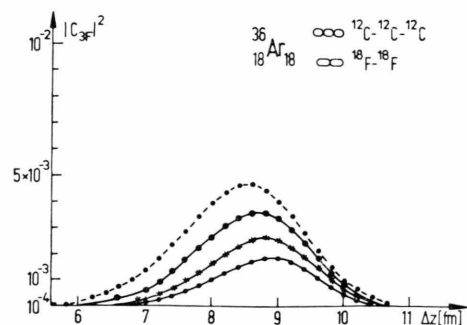


Fig. 7. As Fig. 5 but for the ground state of $^{12}\text{C} - ^{12}\text{C} - ^{12}\text{C}$: $|C_{3\text{F}}|^2 = |\langle \Phi_{^{12}\text{C}-^{12}\text{C}-^{12}\text{C}}^0 | \Psi_{^{18}\text{F}-^{18}\text{F}}^0 \rangle|^2$.

above, one may calculate the relative probability of ‘true’ ternary fission of ^{36}Ar .

$$|C_{3\text{F}}|^2 = |\langle \Phi_{12\text{C}-12\text{C}-12\text{C}}^0 | \Psi_{18\text{F}-18\text{F}}^0 \rangle|^2$$

is plotted in Figure 7. Again, the results are as expected: The maximum is about an order of magnitude smaller than the maximal probability for α -fission with the same two-center deformation and the maximum increases as the two fragments get more deformed. – It should be noted that the maximum occurs at a smaller separation of the two ^{18}F s. This is reasonable in light of the results of Diehl et al.¹⁰ who showed (within the liquid drop model) that for light nuclei the paths leading to binary and ternary fission, respectively, will start to diverge from each other very early and far from the (binary) scission point.

For heavy compound nuclei, these scission points are near each other. Hence we expect to find the maximal overlap for the real ternary fission of heavy nuclei to be at about the same place as the maximum for α -fission. For these nuclei, however, the angular momentum dependent corrections have to be taken into account. In addition, the heights of the barriers between the fragments will be important degrees of freedom. Thus, the eigenfunctions of the complete Hamiltonians have to be used.

Our model – even in its most simple form – shows its usefulness. It is now necessary to start with more detailed calculations. We hope to present the comparison of binary, α -ternary, and real ternary fission, and of ternary mass distributions in the near future.

We like to thank the Hochschul-Rechenzentrum of the University Frankfurt for the computertime necessary to perform the numerical calculations.

Appendix

Details of the Calculation of the Overlap

Nucleons are fermions and therefore the total wavefunctions $\Phi(1, 2, \dots, A)$ of an A -nucleon system has to be antisymmetric with respect to an interchange of the N neutrons and the Z protons, respectively. This will certainly be the case, if Φ is the product of two Slater-determinants:

$$\begin{aligned} \bar{\Phi}(1, 2, \dots, A) &= \mathbf{A}_N \mathbf{A}_Z [\varphi_1(1) \\ &\quad \dots \varphi_N(N) \varphi_{N+1}(N+1) \dots \varphi_{N+Z}(N+Z)] \\ &= \frac{1}{N!} \det_N[\varphi_i(j)] \cdot \frac{1}{Z!} \det_Z[\varphi_i(j)], \end{aligned}$$

where \mathbf{A}_N and \mathbf{A}_Z are the antisymmetrization operators for neutrons and protons.

The overlap of two N -neutron- Z -proton functions

$$\begin{aligned} \Phi &= \frac{1}{\sqrt{A!}} \det_A[\varphi_i(j)], \\ \Psi &= \frac{1}{\sqrt{A!}} \det_A[\psi_i(j)], \end{aligned}$$

can be written as

$$\langle \Phi | \Psi \rangle = \det_A(\langle \varphi_i | \psi_j \rangle).$$

Taking

$$\varphi_i = \sum_{v=1}^{N_\varphi} a_{iv} \varphi_v^0, \quad \psi_i = \sum_{\mu=1}^{N_\psi} b_{i\mu} \psi_\mu^0, \quad 1 \leq i \leq A,$$

φ^0 , ψ^0 , N_φ , and N_ψ being defined in Sec. 3, the single-particle overlaps are changed to

$$\langle \varphi_i | \psi_j \rangle = \sum_{v=1}^{N_\varphi} \sum_{\mu=1}^{N_\psi} a_{iv} b_{j\mu} m_{v\mu},$$

where $m_{v\mu} = \langle \varphi_v^0 | \psi_\mu^0 \rangle$. Therefore

$$\begin{aligned} \langle \Phi | \Psi \rangle &= \begin{vmatrix} \sum_{v_1=1}^{N_\varphi} \sum_{\mu_1=1}^{N_\psi} a_{1v_1} b_{1\mu_1} m_{v_1\mu_1} & \dots & \sum_{v_1=1}^{N_\varphi} \sum_{\mu_1=1}^{N_\psi} a_{1v_1} b_{Av_1} m_{v_1\mu_1} \\ \vdots & & \vdots \\ \sum_{v_A=1}^{N_\varphi} \sum_{\mu_A=1}^{N_\psi} a_{Av_A} b_{1\mu_A} m_{v_A\mu_A} & \dots & \sum_{v_A=1}^{N_\varphi} \sum_{\mu_A=1}^{N_\psi} a_{Av_A} b_{A\mu_A} m_{v_A\mu_A} \end{vmatrix} \\ &= \sum_{v_1, \dots, v_A=1}^{N_\varphi} \sum_{\mu_1, \dots, \mu_A=1}^{N_\psi} a_{1v_1} \dots a_{Av_A} \cdot m_{v_1\mu_1} \dots m_{v_A\mu_A} \cdot \hat{B} \begin{pmatrix} 1 & 2 & \dots & A \\ \mu_1 & \mu_2 & \dots & \mu_A \end{pmatrix}; \end{aligned}$$

$$\hat{B} \begin{pmatrix} 1 & 2 & \dots & A \\ \mu_1 & \mu_2 & \dots & \mu_A \end{pmatrix} = \begin{vmatrix} b_{1\mu_1} & b_{1\mu_2} & \dots & b_{1\mu_A} \\ b_{2\mu_1} & b_{2\mu_2} & \dots & b_{2\mu_A} \\ \vdots & \vdots & & \vdots \\ b_{A\mu_1} & b_{A\mu_2} & \dots & b_{A\mu_A} \end{vmatrix}.$$

With the aid of the general Kronecker symbol

$$\delta_{\underbrace{\mu_1 \dots \mu_A}_{\ell_A}} = \begin{cases} +1 \\ 0 \\ -1 \end{cases}$$

if μ_1, \dots, μ_A is $\left\{ \begin{array}{l} \text{an even} \\ \text{no} \\ \text{an odd} \end{array} \right\}$ permutation of $Q_1 < Q_2 < \dots < Q_A$, this can be rewritten to

$$\begin{aligned} \langle \Phi | \Psi \rangle &= \sum_{\nu_1, \dots, \nu_A=1}^{N_\varphi} a_{1\nu_1} \dots a_{A\nu_A} \sum_{1 \leq Q_1 < \dots < Q_A \leq N_\psi} \widehat{B} \left(\begin{array}{c} 1 \dots A \\ Q_1 \dots Q_A \end{array} \right) \sum_{\mu_1, \dots, \mu_A=1}^{N_\psi} \delta_{\mu_1 \dots \mu_A}^{Q_1 \dots Q_A} m_{\nu_1 \mu_1} \dots m_{\nu_A \mu_A} \\ &= \sum_{\nu_1, \dots, \nu_A=1}^{N_\varphi} a_{1\nu_1} \dots a_{A\nu_A} \sum_{1 \leq Q_1 < \dots < Q_A \leq N_\psi} \widehat{B} \left(\begin{array}{c} 1 \dots A \\ Q_1 \dots Q_A \end{array} \right) \widehat{M} \left(\begin{array}{c} \nu_1 \dots \nu_A \\ Q_1 \dots Q_A \end{array} \right). \end{aligned}$$

Similarly,

$$\langle \Phi | \Psi \rangle = \sum_{1 \leq Q_1 < \dots < Q_A \leq N_\psi} \widehat{B} \left(\begin{array}{c} 1 \dots A \\ Q_1 \dots Q_A \end{array} \right) \sum_{1 \leq \sigma_1 < \dots < \sigma_A \leq N_\varphi} \widehat{M} \left(\begin{array}{c} \sigma_1 \dots \sigma_A \\ Q_1 \dots Q_A \end{array} \right) \sum_{\nu_1, \dots, \nu_A=1}^{N_\varphi} \delta_{\sigma_1 \dots \sigma_A}^{\nu_1 \dots \nu_A} a_{1\nu_1} \dots a_{A\nu_A}$$

which finally leads to

$$\langle \Phi | \Psi \rangle = \sum \widehat{A} \left(\begin{array}{c} 1 \ 2 \ \dots \ A \\ \sigma_1 \ \sigma_2 \ \dots \ \sigma_A \end{array} \right) \widehat{B} \left(\begin{array}{c} 1 \ 2 \ \dots \ A \\ Q_1 \ Q_2 \ \dots \ Q_A \end{array} \right) \widehat{M} \left(\begin{array}{c} \sigma_1 \ \sigma_2 \ \dots \ \sigma_A \\ Q_1 \ Q_2 \ \dots \ Q_A \end{array} \right),$$

where the sum goes over all $\binom{N_\varphi}{A}$ combinations $1 \leq \sigma_1 < \dots < \sigma_A \leq N_\varphi$ and all $\binom{N_\psi}{A}$ combinations $1 \leq Q_1 < \dots < Q_A \leq N_\psi$.

Overlap between Basis Functions

Each base energy will be represented by two wave functions that differ only in their spin functions $v_{m_s}(s)$. If m_s is different for φ_ν^0 and ψ_μ^0 , $\langle \varphi_\nu^0 | \psi_\mu^0 \rangle = 0$.

Therefore, \widehat{M} has the following structure, assuming N_φ and N_ψ are even,

$$\widehat{M} = \begin{vmatrix} m_{11} & 0 & m_{13} & 0 & \dots & m_{1(N_\varphi-1)} & 0 \\ 0 & m_{22} & 0 & m_{24} & \dots & 0 & m_{2N_\varphi} \\ \vdots & & & & & & \\ m_{(N_\varphi-1)1} & 0 & m_{(N_\varphi-1)3} & 0 & \dots & m_{(N_\varphi-1)(N_\varphi-1)} & 0 \\ 0 & m_{N_\varphi 2} & 0 & m_{N_\varphi 4} & \dots & 0 & m_{N_\varphi N_\varphi} \end{vmatrix}.$$

The elements connected by a bar are equal. In general, we have

$$\begin{aligned} m_{(2\nu-1)2\mu} &= m_{2\nu(2\mu-1)} = 0, \\ m_{(2\nu-1)(2\mu-1)} &= m_{2\nu 2\mu}, \\ \nu &\in \{1, 2, \dots, N_\varphi/2\}, \quad \mu = \{1, 2, \dots, N_\psi/2\}. \end{aligned}$$

If φ_ν^0 and ψ_μ^0 have different quantum numbers n_φ , $\langle \varphi_\nu^0 | \psi_\mu^0 \rangle = 0$. This means that the determinant of a minor of \widehat{M} will vanish, if any $\varphi_{\sigma_i}^0$ has a quantum number n_φ that is not also the quantum of at least one of the $\psi_{\varrho_j}^0$.

Furthermore, any minor $\widehat{M} \left(\begin{array}{c} \sigma_1 \dots \sigma_A \\ Q_1 \dots Q_A \end{array} \right)$ will vanish, if the number of base functions φ_σ^0 that have a certain quantum number \bar{n}_φ is different from the number of functions ψ_ϱ^0 with the same \bar{n}_φ . To see that, let $\varphi_{\sigma_{\nu_1}}^0 \dots \varphi_{\sigma_{\nu_x}}^0$ and $\psi_{\varrho_{\mu_1}}^0 \dots \psi_{\varrho_{\mu_\beta}}^0$ be those func-

tions with the quantum number \bar{n}_φ . We then expand \widehat{M} according to Laplace's rule and get

$$\begin{aligned} \widehat{M} \left(\begin{array}{c} \sigma_1 \dots \sigma_A \\ Q_1 \dots Q_A \end{array} \right) &= \sum_{1 \leq \kappa_1 < \dots < \kappa_x \leq A} \widehat{M} \left(\begin{array}{c} \sigma_{\nu_1} \dots \sigma_{\nu_x} \\ Q_{\kappa_1} \dots Q_{\kappa_x} \end{array} \right) \\ &\quad \cdot \widetilde{M}' \left(\begin{array}{c} \sigma_{\nu_1} \dots \sigma_{\nu_x} \\ Q_{\kappa_1} \dots Q_{\kappa_x} \end{array} \right) \end{aligned} \quad (\text{A1})$$

where \widetilde{M}' is the algebraic complement of \widehat{M} . For $\alpha > \beta$ all \widetilde{M} will vanish, because they always contain at least $(\alpha - \beta)$ functions ψ_ϱ^0 whose n_φ -value will be different from \bar{n}_φ . For $\alpha < \beta$ \widetilde{M}' will vanish for the same reason. Only for $\alpha = \beta$ we get

$$\widehat{M} \left(\begin{array}{c} \sigma_1 \dots \sigma_A \\ Q_1 \dots Q_A \end{array} \right) = \widetilde{M} \left(\begin{array}{c} \sigma_{\nu_1} \dots \sigma_{\nu_x} \\ Q_{\mu_1} \dots Q_{\mu_x} \end{array} \right) \widetilde{M}' \left(\begin{array}{c} \sigma_{\nu_1} \dots \sigma_{\nu_x} \\ Q_{\mu_1} \dots Q_{\mu_x} \end{array} \right)$$

as the only non-vanishing term in (A1).

Using the same arguments for \tilde{M}' as for \hat{M} , it is easy to see that \hat{M} can be expanded into

$$\hat{M} \begin{pmatrix} \sigma_1 \cdots \sigma_A \\ \varrho_1 \cdots \varrho_A \end{pmatrix} = \prod_{n_\varphi} \tilde{M} \begin{pmatrix} \sigma_{\{n_\varphi\}} \\ \varrho_{\{n_\varphi\}} \end{pmatrix},$$

where $\sigma_{\{n_\varphi\}}$ is the subset of those σ_i that belong to the same n_φ and where the product over all n_φ represented in \hat{M} has to be taken.

- ¹ P. B. Vitta, Nucl. Phys. **A 170**, 417 [1971]; I. G. Schröder, Nucl. Phys. **A 195**, 257 [1972].
² I. Halpern, CERN Report 6812, 1963; Y. Boneh, Z. Fraenkel, and I. Nebenzahl, Phys. Rev. **156**, 1305 [1967]; A. Katase, J. Phys. Soc. Jap. **25**, 933 [1968]; G. M. Raisbeck and T. K. Thomas, Phys. Rev. **172**, 1272 [1968].
³ F. Fossati and T. Pinelli, Nucl. Phys. **A 249**, 185 [1975].
⁴ J. Maruhn, Diplomarbeit, Universität Frankfurt am Main 1971; J. Maruhn and W. Greiner, Z. Physik **251**, 431 [1972].

- ⁵ J. M. Eisenberg and W. Greiner, Nuclear Theory 1, North-Holland, Amsterdam 1970, 202.
⁶ F. Dickmann, Phys. Lett. **35 B**, 467 [1971].
⁷ I. Ragnerson, Pro. Int. Conf. on the Properties of Nuclei Far from the Region of Beta-Stability, CERN 70-30, Genf 1970, 847; C. Gustafsson, *ibid.*, 654.
⁸ M. Abramowitz and I. A. Stegun, Handbook of Mathematical Functions, Dover Publications, New York 1968.
⁹ J. Hahn, Diplomarbeit, Universität Frankfurt am Main 1975.
¹⁰ H. Diehl and W. Greiner, Nucl. Phys. **A 229**, 29 [1974].